PD based Robust Quadratic Programs for Robotic Systems

Shishir Kolathaya[1] and Sushant Veer[2]

Abstract— **In this paper, inspired by Proportional-Derivative (PD) control laws, we present a class of Control Lyapunov Function (CLF) based Quadratic Programs (QPs) for robotic systems. Proportional-Derivative (PD) control laws are independent of the robot model, however, they fail to incorporate physical constraints, such as torque saturation. On the other hand, most optimization based control design approaches ensure satisfaction of the physical constraints, but they are sensitive to errors in the robot model. The PD based Quadratic Programs (PD-QPs), presented in this paper, are a first step towards bridging this gap between the PD and the optimization based controllers to bring the best of both together. We derive two versions of PD-QPs: model-based and model-free. Furthermore, for tracking time-varying trajectories, we establish asymptotic stability for the model-based PD-QP, and ultimate boundedness for the model-free PD-QP. The performance of the PD-QPs is evaluated on two robot models: a fully actuated cart-pole and an underactuated 5-DOF biped.**

I. Introduction

Despite great advances in the theory of nonlinear controls, Proportional-Derivative (PD) control laws continue to be the most popular choice in industrial applications, according to a survey conducted by the International Federation of Automatic Control (IFAC) [24, Table 1A]. This overwhelming preference for PD controllers stems from three main reasons: First, PD control laws are model-independent unlike various nonlinear controllers—such as input-output (IO) linearization and backstepping—thereby, avoiding brittleness from modeling errors. Second, PD controllers are intuitive to understand and easy to implement. Finally, PD controllers are accompanied by formal stability guarantees, especially for systems with Lagrangian dynamics [5], [9], [14], [27], [32]; see Table I for a non-exhaustive list of such stability results.

Table 1A in [24] also highlighted an increase in the popularity of model predictive controllers (MPCs) which received the second highest impact ratings, next only to PD controllers. The success of MPCs can be attributed to the advances in computational performance which have enabled optimization solvers to operate in real-time. Some instances of optimization based controllers include QP based control of zero-moment point walkers [18], constrained dynamical systems [23], and QP based state estimation of bipeds [29]. Reference [7] presented the class of controllers designed using rapidly exponentially stabilizing CLF-QPs [3], which were successful in realizing stable walking on the limit-cycle gait bipedal robot MABEL. However, these CLF-QPs were derived from input-output linearization based control laws [11, Chapter 13.2], which involve inverting the model, leading to a possible amplification of small modeling errors.

Control Law	Literature
PD regulation	GAS [14], [25], LES [5], [15], GES [17]
PD tracking	LES [10], [16], [27], [28]

TABLE I: A collection of stability results for PD based control of robotic systems. The abbreviations used in the table are given as follows: GAS is globally asymptotically stable; LES is locally exponentially stable; and GES is globally exponentially stable.

With a view toward addressing the limitations of input-output linearization based QPs (IO-QPs), we propose the use of a new class of QPs motivated by PD control laws for robotic systems [6], [14], [21], [28]. We derive two types of PD based QPs (PD-QPs): 1) Model based PD-QP that uses the robot model, and model-free PD-QP that does not require the robot model. For the model based PD-QP, we establish guarantees of asymptotic stability, and for the model-free PD-QP, we establish ultimate boundedness for fully actuated systems. This ultimate bound can be shrunk arbitrarily by tuning the parameters of the QP appropriately, thereby, rendering this class of controllers practically feasible; see Theorem 1 and Remark 1 ahead. We also provide QP formulations for underactuated systems, the stability of which requires a detailed analysis of the zero dynamics; due to space constraints this stability analysis will be presented in a future publication. These QP formulations are validated and compared with IO-QPs for two robot models: fully actuated cart-pole system, and an underactuated 5-DOF biped. Our results show that the PD-QPs are robust even to a 200% increase in the inertial parameters (i.e., three times the actual values), while IO-QP fails with large excursions from the desired trajectories.

The paper is structured as follows. Section II provides a brief technical discussion on CLFs and the associated CLF-QPs. Section III describes the robot model. Sections IV and V contain the main results of the paper, i.e., model-based QP and model-free QP for robotic systems, respectively. Finally, Section VI discusses the simulation results.

Notation. Let $\mathbb{R}$ denote the set of real numbers and $\mathbb{R}^n$ denote the Euclidean space of dimension n. An open Euclidean ball of radius $r > 0$ centered at $x \in \mathbb{R}^n$ is denoted by $\mathbb{B}_r(x)$. For any $x \in \mathbb{R}^n$, the Euclidean norm is denoted by $|x|$, and for any matrix $A \in \mathbb{R}^{n\times m}$, the matrix norm is represented

*This work is supported by DST INSPIRE Fellowship IFA17-ENG212, and Robert Bosch Center for Cyber Physical Systems.

[1]S. Kolathaya is with the Robert Bosch Center for Cyber Physical Systems, Indian Institute of Science, Bengaluru, India. email: shishirk at iisc.ac.in

[2]S. Veer is with the Department of Mechanical and Aerospace Engineering, Princeton University, Princeton, NJ, USA. e-mail: sveer at princeton.edu

by $\|A\|$. The superscript $+$ is used to denote the generalized inverse of a matrix, i.e., the generalized inverse of A is given by A^+. A continuous function $\alpha : \mathbb{R}_{\geq 0} \to \mathbb{R}_{\geq 0}$ is said to belong to class $\mathscr{K}$ if it is strictly increasing and $\alpha(0) = 0$. We say that a function $h : \mathbb{R}^n \to \mathbb{R}^m$ is locally Lipschitz at $x \in \mathbb{R}^n$ if there exist constants $L > 0$ and $r > 0$ such that $\|h(y) - h(x)\| \leq L\|y - x\|$ for all $y \in \mathbb{B}_r(x)$.

II. Technical Prerequisites for CLF-QPs

In this section, we will define a control Lyapunov function (CLF) and the associated quadratic program (QP) for a nonlinear system with affine control.

Given the state[1] $x \in \mathbb{R}^n$ and inputs $u \in \mathscr{U} \subseteq \mathbb{R}^m$, we have the following dynamical system

$$\dot{x} = f_e(t,x) + g_e(t,x)u, \tag{1}$$

where $f_e : \mathbb{R}_{\geq 0} \times \mathbb{R}^n \to \mathbb{R}^n$, $g_e : \mathbb{R}_{\geq 0} \times \mathbb{R}^n \to \mathbb{R}^{n \times m}$ are locally Lipschitz. Intuitively, a CLF ensures the existence of a feedback control law for which the equilibrium of the dynamics are asymptotically stable. In the next definition, we make this notion mathematically precise.

Definition 1: *A continuously differentiable function $V : \mathbb{R}_{\geq 0} \times \mathbb{R}^n \to \mathbb{R}_{\geq 0}$ is said to be a local control Lyapunov function if there exist class $\mathscr{K}$ functions $\alpha_1, \alpha_2, \alpha_3, \alpha_4$, a set of inputs $\mathscr{U} \subseteq \mathbb{R}^m$, and $r > 0$ such that for all $x \in \mathbb{B}_r(0)$,*

$$\alpha_1(|x|) \leq V(t,x) \leq \alpha_2(|x|) \tag{2}$$

$$\left|\frac{\partial V(t,x)}{\partial x}\right| \leq \alpha_3(|x|)$$

$$\inf_{u \in \mathscr{U}} \left[\frac{\partial V(t,x)}{\partial t} + L_{f_e}V(t,x) + L_{g_e}V(t,x)u\right] \leq -\alpha_4(|x|), \tag{3}$$

where $L_{f_e}V, L_{g_e}V$ are the Lie derivatives[2] of V with respect to f_e, g_e, respectively.

Definition 1 is reminiscent of the criterion for Lyapunov's theorem [11, Theorem 4.1], albeit with the control input u. Indeed, choosing a u that satisfies (3) at each time instant results in a closed-loop system for which the CLF, V, acts as a Lyapunov function, ensuring asymptotic stability of the equilibrium point. Conversely, if the closed-loop dynamics of a controller $u = k(t,x)$ exhibits a Lyapunov function for an equilibrium point, then that Lyapunov function is also a CLF as it implicitly ensures the existence of a u that satisfies (3). This observation is formalized in the following lemma:

Lemma 1: *Consider the dynamical system given by* (1). *Let $k : \mathbb{R}_{\geq 0} \times \mathbb{R}^n \to \mathscr{U} \subseteq \mathbb{R}^m$ be a locally Lipschitz control law for which $x = 0$ is an asymptotically stable equilibrium point. Further, let $V : \mathbb{R}_{\geq 0} \times \mathbb{R}^n \to \mathbb{R}_{\geq 0}$ be a Lyapunov function for the closed-loop system obtained by using $u = k(t,x)$ in* (1)*. Then, V is also a CLF for this system.*

Proof of Lemma 1 is obtained directly from Definition 1. With Lemma 1, the search for a CLF reduces to finding a Lyapunov function for *some* stabilizing control law, which—despite being a challenging task in itself—is more tractable than finding a CLF directly.

The ability to forge control laws using a QP with a notion of (inverse) optimality is precisely the reason behind the popularity of CLF based QPs. Therefore, having obtained a CLF from a stabilizing control law, we have a QP based control with (3) as the linear constraint:

$$u^*(t,x) = \arg\min_u \quad u^T H(t,x)u + c(t,x)^T u \qquad \text{(QP)}$$
$$\text{s.t.} \quad \psi_0(t,x) + \psi_1(t,x)u \leq 0,$$

where

$$\psi_0(t,x) = \frac{\partial V(t,x)}{\partial t} + L_{f_e}V(t,x) + \alpha_4(|x|) \tag{4}$$

$$\psi_1(t,x) = L_{g_e}V(t,x), \tag{5}$$

where $H(t,x) \in \mathbb{R}^{m \times m}$ is a positive semi-definite matrix for all t,x, and $c(t,x) \in \mathbb{R}^m$ is a vector contributing to the linear cost. The cost function of (QP) pertains to the energy cost of the control action, while the inequality constraint encapsulates its effect on the stability of the equilibrium. We denote the set of control inputs that satisfy the inequality constraint of (QP) as

$$\mathbf{K}(t,x) = \{u \in \mathscr{U} : \psi_0(t,x) + \psi_1(t,x)u \leq 0\}. \tag{6}$$

III. Robot Model

Consider an n-DOF robotic system with the configuration manifold $\mathbf{Q}$. Let the configuration of the robot be denoted by q, which is a set of coordinates on $\mathbf{Q}$, and let $\dot{q}$ be the rate-of-change of the configuration q. Further, let the state of the system be denoted by[3] $x := (q, \dot{q}) \in T\mathbf{Q} \subseteq \mathbb{R}^{2n}$, where $T\mathbf{Q}$ is the tangent bundle of $\mathbf{Q}$. Then, the Euler-Lagrangian dynamics of the robotic system is given by

$$D(q)\ddot{q} + C(q,\dot{q})\dot{q} + G(q) = Bu, \tag{7}$$

where $D(q) \in \mathbb{R}^{n \times n}$ is the positive-definite inertia matrix, $C(q,\dot{q}) \in \mathbb{R}^{n \times n}$ is the Coriolis-centrifugal matrix, $G(q) \in \mathbb{R}^n$ is the vector of gravity terms, $u \in \mathbb{R}^m$ is the vector of control inputs, and $B \in \mathbb{R}^{n \times m}$ is the mapping of the control inputs to the configuration coordinates. The dynamics (7) can alternatively be expressed in the state-space form as

$$\dot{x} = f(x) + g(x)u, \tag{8}$$

where f, g are appropriately obtained. We assume that the choice of q is such that the mapping of the control inputs to the actuated coordinates is one-to-one, i.e., each column of B consists of only one element with value one and the rest are zeros. We have the following properties of the model [8]:

Property 1: D is positive definite symmetric, and $\dot{D} - 2C$ is skew-symmetric.

[1] The state space dimension will be changed to $2n$ for the robot model later on.

[2] See [21, Chapter 7, 2.1] for a definition of the Lie derivatives.

[3] With an abuse of notation we reuse x from Section II

Property 2: There exist positive constants c_l, c_u, such that for any[4] $(q,\dot{q}) \in T\mathbf{Q}$,

- $c_l \leq \|D(q)\| \leq c_u$
- $c_l \leq \|D^{-1}(q)\| \leq c_u$
- $\|\dot{D}(q)\| \leq c_u|\dot{q}|$
- $\|C(q,\dot{q})\| \leq c_u|\dot{q}|$
- $|G(q)| \leq c_u$.

Note that each of the matrices, D, D^{-1}, C, G have their own upper bounds. We have used the same constants for ease of notations in the ensuing results (see for example, proof of Theorem 1).

A. Error/output dynamics

For a fully actuated robotic system ($m = n$), we are interested in tracking of time and state based desired configuration: $q_d(t,q) : \mathbb{R}_{\geq 0} \times \mathbf{Q} \to \mathbf{Q}$. We assume that the desired trajectory q_d is sufficiently smooth and bounded and that its first $\frac{\partial q_d}{\partial t}$, and second $\frac{\partial^2 q_d}{\partial t^2}$ time derivatives are also uniformly bounded. The error between a configuration q and the desired configuration q_d at a given time t is defined as

$$e(t,q) := q - q_d(t,q). \tag{9}$$

Differentiating (9) with respect to time gives

$$\dot{e}(t,q,\dot{q}) = J_e(t,q)\dot{q} - \frac{\partial q_d(t,q)}{\partial t}, \tag{10}$$

where J_e is the Jacobian matrix of dimension $n \times n$. We will restrict our attention to q_d for which J_e is bounded and invertible. By expressing the configuration and velocities $q, \dot{q}$ in terms of $e, \dot{e}$, we obtain the dynamics as

$$D_e\left(\ddot{e} + \frac{\partial^2 q_d}{\partial t^2}\right) + (C_e + J_d)\left(\dot{e} + \frac{\partial q_d}{\partial t}\right) + G_e = J_e^{-T}u, \tag{11}$$

where $D_e = J_e^{-T} D J_e^{-1}$, $C_e = J_e^{-T} C J_e^{-1} + J_e^{-T} D \frac{d(J_e^{-1})}{dt}$, $G_e = J_e^{-T}G$, $J_d = D_e \frac{\partial}{\partial q}(\frac{\partial q_d}{\partial t}) J_e^{-1}$.

For an underactuated robotic system ($m < n$), we define the following relative degree two outputs:

$$y(t,q) = y_a(q) - y_d(t,q), \tag{12}$$

where $y : \mathbb{R}_{\geq 0} \times \mathbb{R}^n \to \mathbb{R}^m$ is of dimension m. This output is the difference between the actual $y_a : \mathbb{R}^n \to \mathbb{R}^m$ and desired values $y_d : \mathbb{R}_{\geq 0} \times \mathbb{R}^n \to \mathbb{R}^m$. We have the following time-derivatives of the outputs:

$$\dot{y}(t,q,\dot{q}) = J_y(t,q)\dot{q} - \frac{\partial y_d(t,q)}{\partial t}, \tag{13}$$

where J_y is the Jacobian matrix of dimension $m \times n$. Similar to J_e, we restrict our attention to bounded and full-row rank J_y. We obtain the dynamics of the outputs as

$$\ddot{y} - \dot{J}_y\dot{q} + \frac{\partial^2 y_d}{\partial t^2} + \frac{\partial}{\partial q}(\frac{\partial y_d}{\partial t})\dot{q} + J_y D^{-1}(C\dot{q} + G) = J_y D^{-1} B u. \tag{14}$$

[4]This property is always true for robots with pure revolute joints or for robots with all of its prismatic joints preceding the revolute joints [8]. Even for the prismatic joints, like in spring deflections, we know that these deflections are usually restricted by hardstops. This allows us to include a larger class of mechanical systems.

In the next section, we particularize the CLF-QP presented in Section II for the robot model discussed above, leveraging Lyapunov functions developed for PD based control laws.

IV. PD BASED QPs: MODEL DEPENDENT

In this section, we introduce a CLF based QP motivated by PD control laws for robotic systems [6], [14], [21], [28]. Consequently, the resulting QP is referred to as a PD-QP. We will study both fully and underactuated systems. The PD-QPs devised in this section require knowledge of the robot model, however, this is relaxed in Section V.

A. Fully-actuated systems

For the fully actuated robotic system, we have the error dynamics given by (11). It is important to note that the matrices D_e, C_e have similar properties as that of D, C, including Properties 1 and 2; see [21, Chap. 4, Sec. 5.4] for more details. We choose the following PD based CLF candidate motivated from the stability analysis in [28, Appendix]:

$$V(e,\dot{e},q) = \frac{1}{2}e^T K_p e + \frac{1}{2}\dot{e}^T D_e(q)\dot{e} + \alpha(e)e^T D_e(q)\dot{e}, \tag{15}$$

where $K_p \succ 0$ (i.e., a symmetric positive definite matrix of appropriate dimension), and

$$\alpha(e) := \frac{k_0}{1+|e|} = \frac{k_0}{1+\sqrt{e^T e}}, \tag{16}$$

where $k_0 \geq 0$ is a small non-negative number chosen such that V is positive definite. For example, we can choose k_0 that satisfies

$$k_0 \leq \frac{\sqrt{\|K_p\|\|D_e\|}}{\|D_e\|}. \tag{17}$$

Using (4) and (5) on the V in (15), we can choose the following explicit forms for ψ_0 and ψ_1:

$$\begin{aligned}\psi_0 &= \left(\alpha(e)e^T + \dot{e}^T\right)\Bigg(K_p e + K_d\dot{e} - D_e\frac{\partial^2 q_d}{\partial t^2} \\ &\qquad\qquad - (C_e + J_d)\frac{\partial q_d}{\partial t} - J_d\dot{e} - G_e\Bigg) \\ \psi_1 &= \left(\alpha(e)e^T + \dot{e}^T\right)J_e^{-T},\end{aligned} \tag{18}$$

with $K_d \succ 0$. The resulting QP, indeed, yields a feasible solution, as can be verified by taking

$$u = -J_e^T\left(K_p e + K_d\dot{e} - D_e\frac{\partial^2 q_d}{\partial t^2} - (C_e + J_d)\frac{\partial q_d}{\partial t} - J_d\dot{e} - G_e\right),$$

which satisfies the inequality constraint of (QP) with ψ_0 and ψ_1 given by (18). With this inequality, we obtain the derivative $\dot{V}$ as

$$\dot{V} = -\begin{bmatrix} e \\ \dot{e} \end{bmatrix}^T \begin{bmatrix} \alpha K_p & \frac{\alpha K_d - \dot{\alpha} D_e - \alpha \dot{D}_e}{2} \\ \frac{\alpha K_d - \dot{\alpha} D_e - \alpha \dot{D}_e}{2} & K_d - \alpha D_e \end{bmatrix} \begin{bmatrix} e \\ \dot{e} \end{bmatrix}, \tag{19}$$

and the matrix in (19) can be ensured to be positive definite by choosing a small enough k_0 in α (possibly smaller than the previously determined k_0). This establishes asymptotic stability of $(e,\dot{e})$.

It is worth nothing that if $k_0 = 0$, then the resulting $\dot{V}$ in (19) is negative semi-definite, thereby satisfying the conditions of a *weak* form of a Lyapunov function. In fact, for a constant desired configuration, this weak form can be used to establish asymptotic stability for the PD based control law of the form

$$u_{PDG}(e,\dot{q}) = -K_p e - K_d \dot{q} + G(e+q_d), \tag{20}$$

by LaSalle's invariance principle; see [21, Chapter 4, Proposition 4.9] for more details.

B. Underactuated systems

For underactuated systems, since m is the degree of actuation (DOA) with $m<n$, we have the corresponding degree of underactuation as $l=n-m$. To compute suitable control laws to drive $y,\dot{y}\to 0$, we will be mainly using the projection methods developed in [2]. These methods were also used in [12] for operational space control, and in [13] for whole body behaviors. We first replace the terms Bu in (14) by

$$Bu = (\mathbf{1} - N[(\mathbf{1}-BB^T)N]^+)J_y^T F \tag{21}$$

where

$$N = (\mathbf{1} - J_y^T(J_y D^{-1} J_y^T)^{-1} J_y D^{-1}), \tag{22}$$

F is an auxiliary input in the output space, and the superscript $+$ denotes the Moore-Penrose pseudo-inverse. The formulation (21) is such that the first l rows are zero (to be consistent with the underactuation). More details on the significance of F and N can be found in [19, (18)]. With the new F, (14) is reformulated as

$$D_y\ddot{y} + C_y\dot{q} + J_{y_d}\dot{q} + G_y + D_y\frac{\partial^2 y_d}{\partial t^2} = F, \tag{23}$$

where $D_y = (J_y D^{-1} J_y^T)^{-1}$, $C_y = D_y J_y D^{-1} C - D_y \dot{J}_y$, $J_{y_d} = \frac{\partial}{\partial q}(\frac{\partial y_d}{\partial t})$, and $G_y = D_y J_y D^{-1} G$. It is evident that the dynamics in (23) is similar to (11). Therefore, we choose the following V for the underactuated system:

$$V(y,\dot{y},q) = \frac{1}{2}y^T K_p y + \frac{1}{2}\dot{y}^T D_y(q)\dot{y} + \alpha(y) y^T D_y(q)\dot{y}. \tag{24}$$

With this choice of V, we obtain a cost for F, along with the functions ψ_0,ψ_1, which are obtained as

$$\begin{aligned}\psi_0 = (\alpha(y)y^T + \dot{y}^T)\big(K_p y + K_d\dot{y} + \dot{D}_y\dot{y} \\ -(C_y + J_{y_d})\dot{q} - G_y - D_y\frac{\partial^2 y_d}{\partial t^2}\big) \\ \psi_1 = (\alpha(y)y^T + \dot{y}^T),\end{aligned} \tag{25}$$

for which a feasible solution is given by

$$F = -\left(K_p y + K_d\dot{y} + \dot{D}_y\dot{y} - (C_y + J_{y_d})\dot{q} - G_y - D_y\frac{\partial^2 y_d}{\partial t^2}\right).$$

V. PD based QPs: Model Independent

In this section we will focus on QP formulations that do not depend on the model. Similar to the previous section, we will first study fully actuated systems.

A. Fully actuated systems

In order to realize a model-free QP, we need a formulation different than (18) that avoids the use of D_e, C_e, J_d, G_e. Therefore, we consider the following forms for ψ_0,ψ_1:

$$\begin{aligned}\psi_0 &= (\alpha(e)e^T + \dot{e}^T)(K_p e + K_d\dot{e}) \\ \psi_1 &= (\alpha(e)e^T + \dot{e}^T)J_e^{-T}.\end{aligned} \tag{26}$$

The feasibility of the resulting QP can be verified by the control law,

$$u_{PD}(e,\dot{e}) = -K_p e - K_d\dot{e}, \tag{27}$$

which satisfies the inequality in (QP) with the above choice of ψ_0 and ψ_1. The intuition behind the choice of ψ_0 and ψ_1 in (26) and the stability implications of the resulting QP based control law are discussed in the following theorem.

Theorem 1: *Consider the dynamical system given by* (11)*, and the set of control inputs* $\mathbf{K}$ *in* (6) *with* ψ_0,ψ_1 *given by* (26)*. Then for all locally Lipschitz control laws* $k(t,e,\dot{e}) \in \mathbf{K}(t,e,\dot{e})$*, the resulting closed loop system obtained from* (1) *is uniformly ultimately bounded.*

Proof: Given that $\frac{\partial q_d}{\partial t}, \frac{\partial^2 q_d}{\partial t^2}$ are uniformly bounded, we have that

$$\begin{aligned}\left\|D_e\frac{\partial^2 q_d}{\partial t^2}\right\| \le c_q, \quad \left\|(C_e + J_d)\frac{\partial q_d}{\partial t}\right\| \le c_q(|\dot{e}|+1), \\ \|G_e\| \le c_q, \quad \|\dot{D}_e\dot{e}\| \le c_q|\dot{e}|(|\dot{e}|+1),\end{aligned} \tag{28}$$

for some $c_q>0$. Let V be as expressed in (15). For ease of derivation, we will separate the expression in V as

$$V_0 = \frac{1}{2}e^T K_p e + \frac{1}{2}\dot{e}^T D_e\dot{e}, \quad V_c = \alpha(e)e^T D_e\dot{e}. \tag{29}$$

We obtain the derivatives as

$$\begin{aligned}\dot{V}_0 &\le e^T K_p\dot{e} + \dot{e}^T J_e^{-T}u + c_q|\dot{e}|^2 + 3c_q|\dot{e}| \\ \dot{V}_c &\le \alpha e^T J_e^{-T}u + 4c_q|\dot{e}|^2 + 3c_q|\dot{e}| + 2\alpha c_q|e|.\end{aligned} \tag{30}$$

Adding the inequalities in (30) we obtain

$$\dot{V} \le e^T K_p\dot{e} + 6c_q|\dot{e}| + 5c_q|\dot{e}|^2 + 2\alpha c_q|e| + (\alpha e^T + \dot{e}^T)J_e^{-T}u.$$

Substituting for $(\alpha e^T + \dot{e}^T)J_e^{-T}u$ via the inequality constraint given by (26), we obtain

$$\dot{V} \le -\alpha e^T K_p e - \dot{e}^T K_d\dot{e} - \alpha e^T K_d\dot{e} + k_1|\dot{e}|^2 + k_2|\dot{e}| + \alpha k_3|e|, \tag{31}$$

where $k_1 = 5c_q, k_2 = 6c_q, k_3 = 2c_q$. For convenience, we will choose diagonal matrices for K_p, K_d with the scalar gains as k_p, k_d respectively. Using the inequality $-w^2 + wv \le -\frac{w^2}{2} + \frac{v^2}{2}$ in (31), we have

$$\dot{V} \le -\alpha\frac{1}{2}\begin{bmatrix}|e|\\|\dot{e}|\end{bmatrix}^T \underbrace{\begin{bmatrix}k_p & k_d\\ k_d & \frac{k_d-k_1}{\alpha}\end{bmatrix}}_{\Lambda} \begin{bmatrix}|e|\\|\dot{e}|\end{bmatrix} + \frac{k_2^2}{2(k_d-k_1)} + \frac{\alpha k_3^2}{2k_p}. \tag{32}$$

Checking the positivity of the leading principal minors of Λ, we can ensure that $\Lambda \succ 0$ by choosing a k_0 satisfying $0 < k_0 < k_p(k_d-k_1)/k_d^2$, which is a parameter in α, defined in (16). ■

Remark 1: *If we choose the following for k_p, k_d, k_0:*

$$k_p = \varepsilon^2, \quad k_d = \varepsilon + k_1, \quad k_0 = \frac{\varepsilon}{\upsilon}, \tag{33}$$

where $\varepsilon > 1$ is a tunable gain, and υ is picked in such a way that $\Lambda \succ 0$ in (32), we have the following:

$$\dot{V} \leq -\frac{\varepsilon \lambda_{\min}(\Lambda)}{\upsilon(1+|e|)}|(|e|,|\dot{e}|)|^2 + \frac{k_2^2}{2\varepsilon} + \frac{k_3^2}{2\upsilon\varepsilon(1+|e|)}. \tag{34}$$

Given the initial state $(e(0), \dot{e}(0))$ and the corresponding level set of V, we can pick the largest value of $|e|$ in this sublevel set of V. By choosing a large enough ε, we can arbitrarily shrink the constant terms in (34) to a small enough value, resulting in smaller ultimate bounds.

B. Underactuated systems

In Section IV-B, we studied underactuated systems and formulated the model based QP that yield asymptotic convergence of the outputs of the robot. This QP computes F, which is transmitted to the actuators through a model-based mapping; see (21). Due to space constraints, we will only study tracking of time varying trajectories, in particular, outputs (12) of the following form:

$$y_t(q^a, t) := q^a - q_d^a(t), \tag{35}$$

where the actual values are the actuated configuration q^a, and the desired values $q_d^a : \mathbb{R}_{\geq 0} \to \mathbb{R}^m$ are only dependent on time. Similar to q_d for fully actuated systems, we assume that $q_d^a, \dot{q}_d^a, \ddot{q}_d^a$ are all bounded by a constant $c_q > 0$. With these outputs, we can use formulations analogous to (26) for ψ_0, ψ_1 to obtain

$$\begin{aligned} \psi_0 &= (\alpha(y_t) y_t^T + \dot{y}_t^T)(K_p y_t + K_d \dot{y}_t) \\ \psi_1 &= \alpha(y_t) y_t^T + \dot{y}_t^T. \end{aligned} \tag{36}$$

It is worth noting that due to the coupling between the uncontrolled and controlled states of the robot, we cannot guarantee convergence of the outputs. The stability properties of PD-QPs for underactuated systems will be discussed in future work due to space limitations. In the next section, we will apply the QPs obtained so far on the example models.

VI. Discussion and Simulation Results

In this section we will discuss the simulation results for the various types of QPs described in Section IV and V, and compare them with pertinent CLF-QPs in the literature.

A. Review of CLF-QPs in literature

The CLFs typically used in the literature for robotic systems are by input-output (IO) linearization [3], [20], [22]. For a state dependent relative degree two output y, the IO linearizing control law is of the form:

$$u_{\mathrm{IO}}(q, \dot{q}, \mu) = L_g L_f y(q, \dot{q})^{-1}(-L_f^2 y(q, \dot{q}) + \mu), \tag{37}$$

where L_g, L_f are the Lie derivatives, and $\mu \in \mathbb{R}^m$ is the auxiliary control input. Feedback linearization results in a linear system with μ as the new control input. Based on LQR techniques, we obtain the Lyapunov function for this linear system, V_{IO} [22, eqn. (17)], which yields the IO-QP formulation:

$$\begin{aligned} \min_{\mu} \quad & \mu^T \mu \qquad \text{(IO-QP)} \\ \text{s.t.} \quad & L_f V_{\mathrm{IO}}(q,\dot{q}) + L_g V_{\mathrm{IO}}(q,\dot{q}) u_{\mathrm{IO}}(q,\dot{q},\mu) \leq -\gamma V_{\mathrm{IO}}(q,\dot{q}), \end{aligned}$$

where μ is affine in the inequality constraint (based on (37)). $\gamma > 0$ is obtained from the continuous-time algebraic Riccati equations (CARE) (see [3, eqns. (15)-(18)]). (IO-QP) is evaluated for every state feedback x to yield an auxiliary input $\mu(x)$. On account of the convexity of (IO-QP) for a given x, a unique optimal[5] $\mu(x)$ exists, which is then used to compute $u(x)$ according to (37). Additional constraints, like torque limits, are also included with a relaxation term $\delta > 0$ to the CLF constraint (see [22, Section II.D, (24)]).

Since the IO-QP requires the full model of the system, there are no guarantees of stability under modeling uncertainty. A robust variant of the IO-QP (robust IO-QP) was presented in [22], which, however, requires an estimate of the bound on the modeling errors. If the actual modeling error violates this bound, then the robust IO-QP cannot guarantee convergence, potentially leading to failure. On the other hand, if the estimate of the modeling error bound is chosen too large, then the robust IO-QP may not be feasible. The model independent PD-QP we provide in Section V avoids these issues, primarily, because we do not require an estimate of the modeling uncertainties, i.e., our approach works for *any* bounded modeling errors[6].

B. Cost

Similar to the methodology followed in [18, Section V], we will use a reference input for the cost function in (QP):

$$(u - u_{\mathrm{ref}}(t,q,\dot{q}))^T (u - u_{\mathrm{ref}}(t,q,\dot{q})). \tag{38}$$

For example, we can choose the control law (27) as u_{ref} for our QP formulations. This promotes real-time convergence by keeping the inputs close to a region where the inequality constraints are satisfied, leading to lower computational loads. Note that a straightforward option for the cost function would have been minimization of the torques (i.e., minimizing $u^T u$), but, it was shown in [20, Section VII-A] that this form of QP often suffers from discontinuity due to vanishing constraints. Therefore, the actual CLF based QPs implemented in the robotic systems in [3], [20], and also in [22] were minimizing the difference between u and some u_{ref}[7]. Even [18] utilized cost functions that minimized the difference between the actual and the reference accelerations. A detailed analysis of the choice of cost functions will be the subject of future work.

C. Results and comparison

We will test our controllers on two robot models: 1) a cart-pole system and 2) a 5-DOF biped. A video comparing

[5] Optimality here refers to the solution of (IO-QP), $\mu(x)$, for a *given* x.

[6] It is worth noting that our uncertainty bounds are only on the inertial parameters, and not on the states (as shown by (32)).

[7] Even (IO-QP) minimizes the auxiliary input μ.

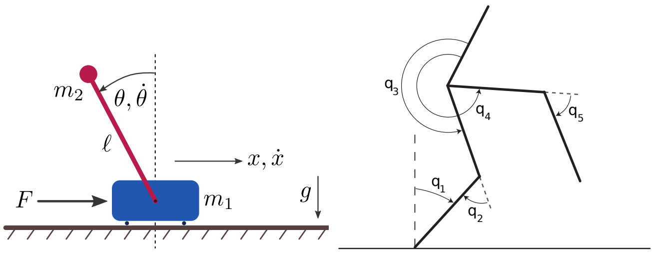

Fig. 1: Figure showing the cart-pole system on the left and a 5-DOF bipedal robot on the right.

the performance of our controllers with those in the existing literature is provided with the submission. A link to the video is also available in [1].

1) Cart-pole system: Fig. 1 shows the cart-pole model with cart having mass $m_1 = 5$kg and the pole having mass $m_2 = 1$kg and length $\ell = 1$m. The states are cart position x, velocity $\dot{x}$ and pole angle θ, velocity $\dot{\theta}$. We have assumed full actuation in order to compare with the traditional QPs existing in literature. The goal is to drive the state vector to zero i.e., $(x, \dot{x}, \theta, \dot{\theta}) \to 0$. Fig. 2 shows the comparison between the traditional IO-QP (given by (IO-QP)), model based PD-QP ((QP) with ψ_0, ψ_1 given by (18)), and model-free PD-QP ((QP) with ψ_0, ψ_1 given by (26)), along with the cost (38). For u_{ref}, we used (27) for both the model based and model-free PD-QPs. Torque and Force limits for all the QPs were set at 100N and 100Nm. Relaxations on the CLF constraint were also introduced to ensure feasibility under torque limits. Table III shows the exact QP formulation used. As shown by Fig. 2, (IO-QP) fails for a 200% increase in the masses m_1 and m_2, while the PD-QPs yield sufficient tracking performances. It can also be observed that large inertial terms introduce larger oscillations, however, these oscillations can be reduced with larger gains.

2) 5-DOF underactuated biped: Fig. 1 shows the stick figure of the bipedal robot used for the simulation. The configuration is given by $q = (q_1, \ldots, q_5)$. The first coordinate, q_1, is the calf angle and is underactuated, while the remaining angles, stance and nonstance knee, stance and nonstance hip, are actuated. Mass and other inertial properties of the robot are provided in [31, Fig. 3b]. Since our focus here is only on continuous dynamics, we will study trajectory tracking control for only one step; an extension to multiple steps would lead to a system with impulse effects that exhibits a periodic orbit under disturbances, the analysis of which can be approached in the manner of [26].

Since the outputs are defined as the difference between the actual and the desired values (12), we will first define the actual outputs y_a for the biped model. The actual outputs (y_a) are given by

$$y_a(q) = \begin{bmatrix} -1 & -1 & -1 & 1 & \frac{L_c}{L_c+L_t} \\ 0 & 1 & 0 & 0 & 0 \\ 0 & 0 & 1 & 0 & 0 \\ 1 & 1 & 1 & 0 & 0 \end{bmatrix} q, \tag{39}$$

where L_c, L_t are the calf and thigh lengths respectively. The rows of y_a correspond to nonstance slope, stance knee angle, nonstance knee angle, and the torso angle of the robot respectively. Due to space constraints, we have only provided the matrix in (39), and a detailed explanation for the individual rows of y_a are found in [4]. The desired outputs y_d are given by the canonical walking functions (CWFs) [4]:

$$y_H(\tau, \alpha) = e^{-\alpha_1 \tau}(\alpha_2 \cos(\alpha_3 \tau) + \alpha_4 \sin(\alpha_3 \tau)) + \alpha_5, \tag{40}$$

where $\alpha_1 - \alpha_5$ are coefficients that are predetermined via an offline optimization [31], [30]. τ is a parameterized function, which is either represented by a monotonically increasing phase variable or a scaled function of time. We will choose the phase variable for the model based QPs, and time for the model-free QP. The phase variable is obtained as

$$\delta p_{\text{hip}}(q) = L_c(-q_1) + L_t(-q_1 - q_2). \tag{41}$$

Since there are four outputs, there are four CWFs yielding the desired outputs as the vector $y_d(t) := [y_H(t, \alpha^1), y_H(t, \alpha^2), \ldots, y_H(t, \alpha^4)]^T$. Here, the superscript for α represents the row index. In order to drive the actual outputs to the desired outputs of the robot, we utilized the model based and model-free PD-QPs presented in this paper for underactuated systems, i.e., (QP) with (25) and (36). The cost chosen was (38) with u_{ref} given by (27). For uniformity, we have used the same cost for both the model based and model-free PD-QPs. In addition, we have implemented (IO-QP) and the robust IO-QP formulations from [22] for comparison. More details about the QP formulations are in Table II and III.

Controller Name	QP	Cost	Model required?
IO-QP	(IO-QP)	$\mu^T \mu$	Yes
Robust IO-QP	See [22, (39)]	$\mu^T \mu$	No
Model based PD-QP	(QP) with (25)	(38)	Yes
Model-free PD-QP	(QP) with (36)	(38)	No

TABLE II: Table showing the list of controllers used on the bipedal robot. It must be noted that Robust IO-QP did not require the model, but required the uncertainty bound to realize convergence.

To validate the proposed PD-QPs, we increased the mass and other inertial properties of the robot by 200% from the inertial properties used to design the controllers. Torque limits of 5Nm along with the CLF relaxations (see Table III) were imposed on all of the controllers listed in Table II. The relaxation term δ has a large penalty value, which ensures that only small violations of the convergence constraint are allowed. However, the ultimate boundedness guarantees may not necessarily be ensured with relaxation, and requires further exploration. It can be observed in Fig. 3 that all of the QPs, except the IO-QP, achieved sufficient tracking for one step. Fig. 4 shows the Lyapunov function and the corresponding torque profiles for both the model-based (top) and the model-free (bottom) PD-QPs for one step. Note that the Lyapunov function shows better convergence and smaller ultimate bound for higher gains.

It is worth noting that, for both the cart-pole and biped models, the model-based and model-free PD-QPs have similar performances (see Fig. 2 and Fig. 3). This is due to

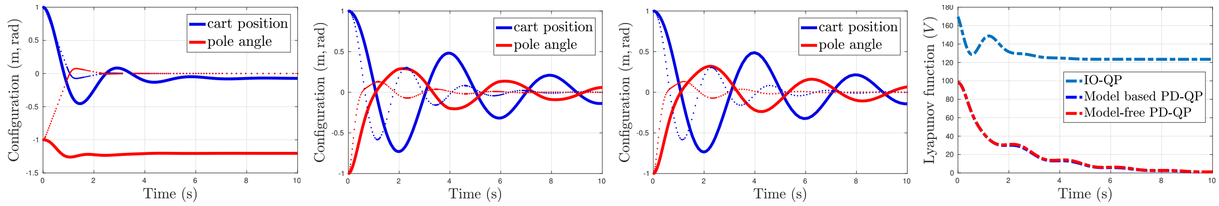

(a) IO-QP (b) Model based PD-QP (c) Model-free PD-QP (d) Lyapunov function

Fig. 2: The left three figures are showing the time response for the cart-pole system. The dotted lines are for a perfect model, and the solid lines are for a 200% model error. IO-QP yields convergence for a perfect model, but does not perform well for the said modeling error. PD-QPs still yield convergence, albeit, with more oscillations due to higher inertia. The right-most figure is showing the Lyapunov functions vs. time for all the three controllers for the 200% model error.

IO-QP (for both cart-pole and biped)

$$\begin{aligned}\min_{\mu,u,\delta}\quad & \mu^T\mu + 1000*\delta^2 \\ \text{s.t.}\quad & L_f V_{\mathrm{IO}}(q,\dot{q}) + L_g V_{\mathrm{IO}}(q,\dot{q})u_{\mathrm{IO}}(q,\dot{q},\mu) \le -\gamma V_{\mathrm{IO}}(q,\dot{q}) + \delta \\ & u = u_{\mathrm{IO}}(q,\dot{q},\mu) \\ & |u| \le 100\,\mathrm{N,Nm} \quad \textbf{cart-pole} \\ & |u| \le 5\,\mathrm{Nm} \quad \textbf{biped}\end{aligned}$$

Model based PD-QP (only used for cart-pole)

$$\begin{aligned}\min_{u,\delta}\quad & (u-u_{\mathrm{ref}}(t,q,\dot{q}))^T(u-u_{\mathrm{ref}}(t,q,\dot{q})) + 1000*\delta^2 \\ \text{s.t.}\quad & (\alpha(e)e^T+\dot{e}^T)\left(K_p e + K_d\dot{e} - D_e\frac{\partial^2 q_d}{\partial t^2} - C_e\frac{\partial q_d}{\partial t} - G_e + J_e^{-T}u\right) \le \delta \\ & |u| \le 100\,\mathrm{N,Nm}\end{aligned}$$

Model based PD-QP (only used for biped)

$$\begin{aligned}\min_{F,u,\delta}\quad & (F-F_{\mathrm{ref}}(t,q,\dot{q}))^T(F-F_{\mathrm{ref}}(t,q,\dot{q})) + 1000*\delta^2 \\ \text{s.t.}\quad & (\alpha(y)y^T+\dot{y}^T)\left(K_p y + K_d\dot{y} + \frac{1}{2}\dot{D}_y\dot{y} - C_y\dot{q} - G_y - D_y\frac{\partial^2 y_d}{\partial t^2} + u\right) \le \delta \\ & Bu = (\mathbf{1} - N[(\mathbf{1}-BB^T)N]^+)J_y^T F \\ & |u| \le 5\,\mathrm{Nm}\end{aligned}$$

Model-free PD-QP (for both cart-pole and biped)

$$\begin{aligned}\min_{u,\delta}\quad & (u-u_{\mathrm{ref}}(t,q,\dot{q}))^T(u-u_{\mathrm{ref}}(t,q,\dot{q})) + 1000*\delta^2 \\ \text{s.t.}\quad & (\alpha(e)e^T+\dot{e}^T)(K_p e + K_d\dot{e}) + (\alpha(e)e^T+\dot{e}^T)J_e^{-T}u \le \delta \quad \textbf{cart-pole} \\ & (\alpha(y)y^T+\dot{y}^T)(K_p y + K_d\dot{y}) + (\alpha(y)y^T+\dot{y}^T)u \le \delta \quad \textbf{biped} \\ & |u| \le 100\,\mathrm{N,Nm} \quad \textbf{cart-pole} \\ & |u| \le 5\,\mathrm{Nm} \quad \textbf{biped}\end{aligned}$$

TABLE III: The QP formulations for the three controllers IO-QP, model based and model-free PD-QPs are shown above. Some of the constraints are applied only to one of cart-pole, biped models, with the appropriate labels included on the side. Video results are shown in the link [1].

the fact that for large enough gains K_p, K_d the nonlinear terms play a small role in the tracking performances. This is observed both in (19) and (32), where the derivatives of the Lyapunov functions are largely influenced by the gain matrices. However, model based PD-QP has lower ultimate bounds than that of the model-free PD-QP, as shown by the Lyapunov functions in Fig. 4.

VII. Conclusions

In this paper, we established methodologies for constructing PD based QPs for robotic systems. PD based control laws are known to exhibit low sensitivity to modeling errors, and are very easy to implement for all kinds of trajectory tracking applications. Capitalizing on this property, we have formulated these PD based control laws in the form of QPs. In addition to providing convergence guarantees for fully actuated systems, we have shown that PD-QPs are robust to scaling of the model parameters of the robot. We have also verified our results in simulation with the two robot models: cart-pole and a 5-DOF biped. Future work will involve developing such PD-QP formulations for a wider class of robotic systems, namely nonholonomic systems, and hybrid robotic systems. We will also study formal stability/boundedness guarantees for underactuated systems.

References

[1] Robustness tests PD-QP. https://youtu.be/_XmlWMwaiOk___.

[2] F. Aghili. A unified approach for inverse and direct dynamics of constrained multibody systems based on linear projection operator: applications to control and simulation. *IEEE Tr. on Robotics*, 21(5):834–849, 2005.

[3] A. D. Ames, K. Galloway, K. Sreenath, and J. W. Grizzle. Rapidly exponentially stabilizing control Lyapunov functions and hybrid zero dynamics. *IEEE Tr. on Automatic Control*, 59(4):876–891, 2014.

[4] Aaron D Ames. Human-inspired control of bipedal walking robots. *IEEE Tr. on Automatic Control*, 59(5):1115–1130, 2014.

[5] S. Arimoto. Stability and robustness of pid feedback control for robot manipulators of sensory capability. *Int. J. of Robotics Research*, pages 783–799, 1984.

[6] S. Arimoto and F. Miyazaki. Asymptotic stability of feedback control laws for robot manipulator. *IFAC Proc. Volumes*, 18(16):221 – 226, 1985. 1st IFAC Symposium on Robot Control.

[7] K. Galloway, K. Sreenath, A. D. Ames, and J. W. Grizzle. Torque saturation in bipedal robotic walking through control lyapunov function based quadratic programs. *IEEE Access*, 3:323–332, 2015.

[8] F. Ghorbel, B. Srinivasan, and M. W. Spong. On the uniform boundedness of the inertia matrix of serial robot manipulators. *J. of Robotic Systems*, 15(1):17–28, 1998.

[9] J. Kasac, B. Novakovic, D. Majetic, and D. Brezak. Global positioning of robot manipulators with mixed revolute and prismatic joints. *IEEE Tr. on Automatic Control*, 51(6):1035–1040, June 2006.

[10] S. Kawamura, F. Miyazaki, and S. Arimoto. Is a local linear pd feedback control law effective for trajectory tracking of robot motion? In *Proc. of IEEE Int. Conf. on Robotics and Automation*, pages 1335–1340 vol.3, 1988.

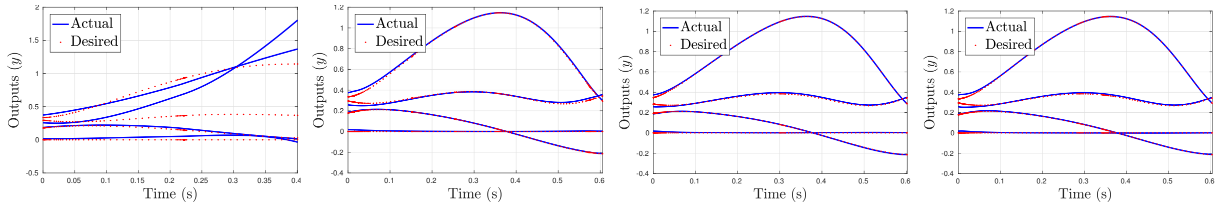

(a) IO-QP (b) Robust IO-QP (c) Model based PD-QP (d) Model-free PD-QP

Fig. 3: Responses for the four types of controllers (see Table II) are shown here for the 5-DOF underactuated biped. The inertial parameters were increased by 200%. It can be observed that the original controller, IO-QP, fails to converge. The other three controllers i.e., Robust IO-QP, Model and model-free PD-QPs are successfully tracking with similar performances.

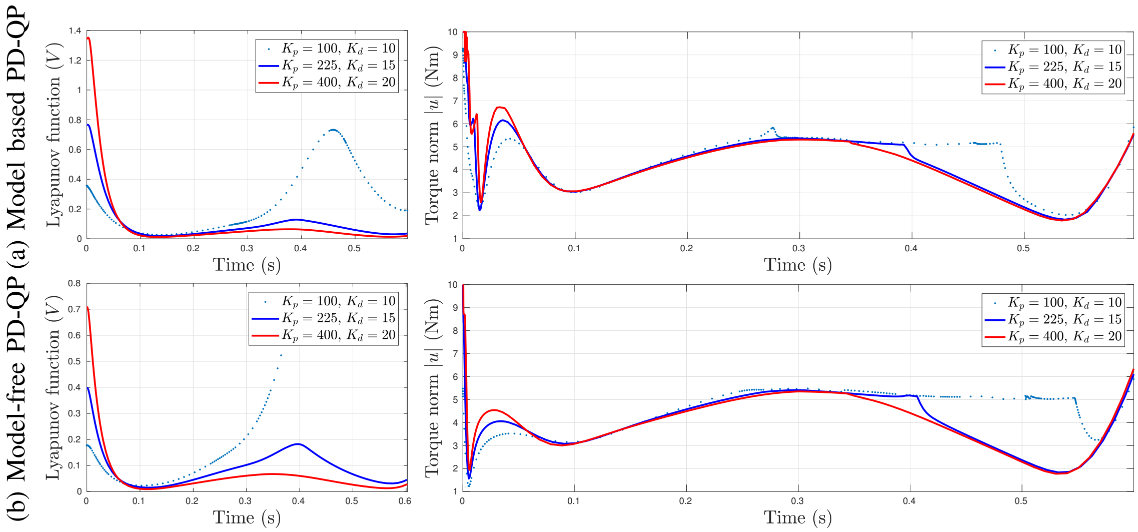

Fig. 4: Figure showing Lyapunov functions (left) and norm of the torques varying (right) as a function of time for the different gains used for both the model based and model-free PD-QPs for the 5-DOF underactuated biped. We observe no convergence for smaller gains, but the bounds reduce as the gains are increased. The torque plots show that the magnitudes marginally increase for increased gains.

[11] H. K. Khalil. *Nonlinear systems*, volume 3. Prentice hall Upper Saddle River, NJ, 2002.

[12] O. Khatib. A unified approach for motion and force control of robot manipulators: The operational space formulation. *IEEE J. on Robotics and Automation*, 3(1):43–53, February 1987.

[13] O. Khatib, L. Sentis, J. Park, and J. Warren. Whole-body dynamic behavior and control of human-like robots. *Int. J. of Humanoid Robotics*, 1(01):29–43, 2004.

[14] D. E. Koditschek. Natural motion for robot arms. In *Proc. of IEEE Conf. on Decision and Control*, volume 23, pages 733–735, 1984.

[15] D. E. Koditschek. Adaptive techniques for mechanical systems. In *Fifth Yale Workshop on Applications of Adaptive Systems Theory, May 1987*, pages 259–265, 1987.

[16] D. E. Koditschek. High gain feedback and telerobotic tracking. In *Proc. of the Workshop on Space Telerobotics*, pages 355–363, 1987.

[17] D. E. Koditschek. Strict global lyapunov functions for mechanical systems. In *Proc. of American Control Conf.*, pages 1770–1775, 1988.

[18] S. Kuindersma, F. Permenter, and R. Tedrake. An efficiently solvable quadratic program for stabilizing dynamic locomotion. In *Proc. of IEEE Int. Conf. on Robotics and Automation*, pages 2589–2594, 2014.

[19] M. Mistry and L. Righetti. Operational space control of constrained and underactuated systems. In *Proc. of Robotics: Science and Systems*, pages 225–232, Los Angeles, CA, USA, 6 2011.

[20] B. J. Morris, M. J. Powell, and A. D. Ames. Continuity and smoothness properties of nonlinear optimization-based feedback controllers. In *Proc. of IEEE Conf. on Decision and Control*, pages 151–158, 2015.

[21] R. M. Murray, Z. Li, and S. S. Sastry. *A Mathematical Introduction to Robotic Manipulation*. CRC Press, Boca Raton, 1994.

[22] Q. Nguyen and K. Sreenath. Optimal robust control for bipedal robots through control Lyapunov function based quadratic programs. In *Proc. of Robotics: Science and Systems*, Rome, Italy, 2015.

[23] M. Posa, S. Kuindersma, and R. Tedrake. Optimization and stabilization of trajectories for constrained dynamical systems. In *Proc. of IEEE Int. Conf. on Robotics and Automation*, pages 1366–1373, 2016.

[24] T. Samad. A survey on industry impact and challenges thereof [technical activities]. *IEEE Control Systems*, 37(1):17–18, Feb 2017.

[25] M. Takegaki and S. Arimoto. A New Feedback Method for Dynamic Control of Manipulators. *Tr. of the ASME J. of Dynamic Systems Measurement and Control*, 103, 1981.

[26] S. Veer, Rakesh, and I. Poulakakis. Input-to-state stability of periodic orbits of systems with impulse effects via Poincaré analysis. *IEEE Tr. on Automatic Control*, 2019.

[27] J. T. Wen and D. S. Bayard. New class of control laws for robotic manipulators part 1. non–adaptive case. *Int. J. of Control*, 47(5):1361–1385, 1988.

[28] L. L. Whitcomb, A. A. Rizzi, and D. E. Koditschek. Comparative experiments with a new adaptive controller for robot arms. *IEEE Tr. on Robotics and Automation*, 9(1):59–70, Feb 1993.

[29] X. Xinjilefu, S. Feng, and C. G. Atkeson. Dynamic state estimation using quadratic programming. In *Proc. of IEEE/RSJ Int. Conf. on Intelligent Robots and Systems*, pages 989–994, 2014.

[30] S. N. Yadukumar, M. Pasupuleti, and A. D. Ames. Human-inspired underactuated bipedal robotic walking with AMBER on flat-ground, up-slope and uneven terrain. In *Proc. of IEEE/RSJ Int. Conf. on Intelligent Robots and Systems*, pages 2478–2483, October 2012.

[31] S. Nadubettu Yadukumar, M. Pasupuleti, and A. D. Ames. *From Formal Methods to Algorithmic Implementation of Human Inspired Control on Bipedal Robots*, pages 511–526. Springer Berlin Heidelberg, Berlin, Heidelberg, 2013.

[32] C. Zheng and Y. Su. PID control of robot manipulators in task space. In *2010 8th World Congress on Intelligent Control and Automation*, pages 1794–1799, July 2010.